PER-CHANNEL COLOR BARCODES FOR DISPLAYS

Karthik Dinesh, Gaurav Sharma

Dept. of Electrical and Computer Engineering, University of Rochester, Rochester, NY

ABSTRACT

We present a per-channel framework for extending monochrome barcodes to color for display applications, offering increased data rates and capacity. Data is independently encoded into barcodes, incorporated within a color image as the red (R), green (G), and blue (B) channels and decoded from the corresponding R, G, and B channels in the image of the displayed barcode captured with a smartphone. Using a physical model for the display and capture processes, we show that the cross-channel interference in this situation is appropriately modeled by a linear mixing relation. Via experiments done over multiple smartphones and displays, we demonstrate that the impact of the interference is small and can be further mitigated through the use of interference cancellation. Two methods are presented for estimating and canceling the interference: either using pilot blocks in coherent designs where the synchronization marker patterns align between the codes or using expectation maximization. Results are presented for both QR and Aztec color codes in this framework, highlighting its versatility. Overall bit error rates are shown to be below 1.23% and are further reduced by interference cancellation. These low error rates are well within the correction capacity of the error correction codes used for typical color barcodes.

***Index Terms*—** Display barcodes, color barcodes, mobile applications, per-channel encoding.

1. INTRODUCTION

Barcodes encode data in a machine readable image format. Conventionally 1-D patterns (vertical lines) were used for barcodes such as the universal product code (UPC)1 [1], but with ready availability of image sensors 2-D barcodes have gained prominence. Most popular and commonly used 2-D barcodes are the QR code [2], Aztec code [3, 4], and Data Matrix [5]. Both 1-D and 2-D barcodes have traditionally been used in printed black-and-white formats. Several recent efforts have focused on color versions of printed barcodes with a view to increasing the capacity per unit area of footprint. The use of color in printed barcodes presents a number of challenges that prior research has addressed through several innovations [6, 7, 8, 9, 10].

In this paper, we focus on display applications of barcodes, and specifically on color barcodes for such applications. While display applications of barcodes are more recent than the long-standing print-based applications, they are becoming increasingly common. Just like their print counterparts, barcodes displayed on electronic displays are increasingly used by users to connect with online sources of information by capturing an image of the displayed barcode with an application installed on their smartphones. Applications of this type include connectivity for advertised content, immediate information access (for instance at transit points), and for encoding boarding pass information displayed on smartphones to automate boarding (Aztec codes are common for this application). The capability for interactivity with display barcodes also enables additional applications [11]. Different barcodes such as Visual Code [12], Spot code [13] and Magneti-Code [14] have been used as visual tags for interaction with large screens. A secured barcode based communication system (SBVLC) [15] has been used for information sharing, secured device pairing, and other security related applications. The use of barcodes has also been proposed for automating point of sale transactions such as checkout payment systems, which are now seeing deployment with the recently announced *Walmart Pay*, a QR code enabled smartphone-based mobile payment system from the US's biggest retailer Walmart [16, 17]. In several of these applications, barcodes are competing with near field communication (NFC) [18] and the closely related radio frequency identification (RFID) tag [19, 20, 21] technologies (See [11] for a recent comparison).

Most barcodes used for display applications have been based on monochrome i.e black and white barcodes. Because, nearly all displays and smartphone cameras today are color-capable, there is no cost or accessibility barriers to using color barcodes instead of the monochrome versions. Compared to monochrome barcodes, color barcodes offer the potential for higher information capacity through better utilization of the available channel from the display to the smartphone camera. For temporal streaming of data between screens and smartphones, two recent efforts [6, 22] have proposed the use of specially designed color display barcodes. The specialized barcode designs, however, target only the specific niche of data streaming, compared to the much broader class of applications typical of standardized barcodes. Also they have only undergone rather limited testing and are missing key features such as robust synchronization capability and forward error correction, features that are necessary for actual deployments and for comparison with already existing monochrome alternatives.

In this paper we present a per channel framework for color barcodes for displays that mirrors and complements our group's recent work [10] on per channel color barcodes for print applications. Compared with alternatives that re-design color barcodes from scratch, the per-channel framework has the significant advantage that it re-uses components already designed and optimized for monochrome barcodes for synchronization, error correction coding, etc, leveraging the tremendous investment that has already been made in optimizing these. The result is a design that is much more robust and ready for use compared to *de novo* constructions. We present the framework and demonstrate that, for display applications, far less color interference is encountered compared to what was observed for print color barcodes. We also present analysis specific to our proposed per channel color barcodes for display which provides an appropriate model for color interference with minimal approximations that provides physical intuition and enables methods for estimation and cancellation for performance improvements. Results for tests conducted with QR and Aztec codes in our framework across multiple displays and smartphones demonstrate that the proposed framework is effective: observed bit error rates are below 1.23% natively, and further decreased upon interference cancellation. Both coherent designs where the synchronization marks are aligned between the individual channel barcodes and incoherent designs that do not exhibit these constraints are shown to perform well in the proposed framework.

The paper is organized as follows: In Section 2 we present the per-channel framework for display color barcodes. Data encoding, decoding, and cross-channel interference are discussed and by using a physical model for the display and capture process we show that cross channel interference can be modeled by a linear mixing relation. We show a visual demonstration of the typical color interference and propose methods for estimation and cancellation of this interference motivated by our work on printed color barcodes: specifically, using pilot blocks [10] or an EM approach [23]. Experimental setup, tests, and results are presented in Section 3. The paper concludes with a summary and discussion in Section 4.

2. PER-CHANNEL DISPLAY COLOR BARCODES

2.1. Data Encoding and Decoding

Independent messages m_1, m_2, m_3 are encoded as three individual monochrome barcodes that are placed in the three R, G, and B channels, respectively, of a color image, thereby forming our per-channel color barcode. Fig.1 illustrates this process. Encoding of messages in monochrome barcodes also typically incorporates error correction coding (at a suitably chosen level) which helps in error recovery during data extraction from captured barcode images. The resulting color barcode is displayed on regular RGB display.

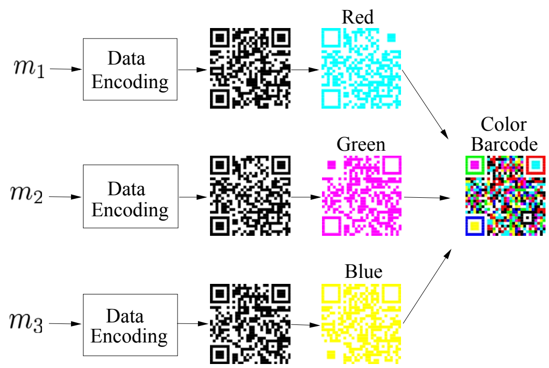

Fig. 1: Per-Channel encoding for color display barcodes. (Coherent design)

An image of the displayed color barcode is captured using a cell phone camera and used to attempt recovery of the encoded data using the process outlined in Fig.2. The captured image is divided into the red (R), green (G), and blue (B) channels used for the capture. In an ideal situation, the camera R, G, and B channels capture only the variation in the corresponding display R, G, and B channels and there is no impact of displayed channel on non-matching capture channels. Under this ideal situation, R, G, and B channels form three noninteracting parallel channels carrying independent data streams and the data is extracted from the R, G, and B capture channels just as it would be for a monochrome barcode. In practice, however, the individual channels of the captured image can include contributions from images in channels other than the matching display channel, a phenomenon we refer to as cross channel interference. The effect of interference is demonstrated in Fig.3 (please see electronic version). We see that cross channel interference is relatively small and restricted largely to the green channel. This cross channel interference sometimes results in decoding failure when the captured image is directly fed into the decoder software. We therefore consider a

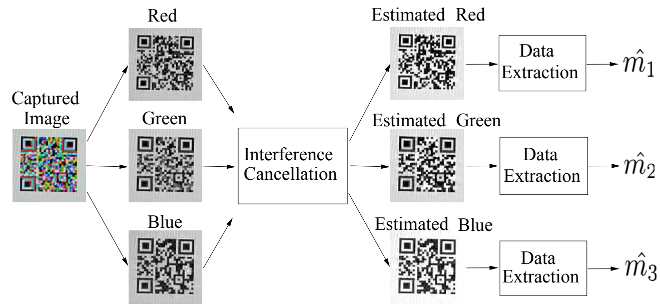

Fig. 2: Data decoding from a captured image of a displayed per-channel barcode. (Incoherent design)

physical model for the display and capture process in the following section, which allows us to parameterize the cross channel interference as a linear 3×3 mixing matrix, which we can estimate and use to cancel the interference. The development shares similarities with our work for printed color barcodes in [10], although the models and the methodology are different due to the inherently different physics of displays and printers.

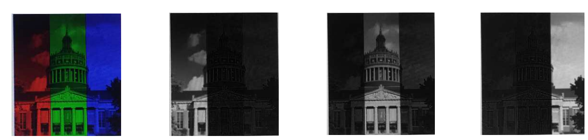

a) RGB Stripes b) R Channel c) G Channel d) B Channel

Fig. 3: Image demonstrating cross channel interference encountered in the per-channel framework. Subfigure (a) shows a displayed image consisting of three stripes with only one of the R, G and B channel active in each stripes. Subfigures (b), (c) and (d) show the R, G and B channels respectively, of a photograph of the displayed image taken with a smartphone.(See electronic version of image).

2.2. Physical model for display-capture process

Modeling the display-capture process enables us to understand the cross channel color interference in a better way and develop methods for mitigating its impact. Color displays are additive devices where the displayed spectrum at each pixel can be modeled as linear combination of the spectrum of R, G, B channels of the display [24] which we denote by $P_i(\lambda)$, $i \in \{R, G, B\}$ with the coefficients of the linear combinations determined by the image being displayed. We represent the displayed color barcode as three binary images $I_i^d(x, y)$ with $i \in \{R, G, B\}$ corresponding, respectively, to the R, G, and B channels with (x, y) denoting the pixel co-ordinates. $I_i^d(x, y)$ is '1' when one of the R, G, or B display channel is turned on and '0' when off. The spatial spectral distribution of the displayed pattern is then given as

$$r(x, y; \lambda) = \sum_{i \in \{R,G,B\}} I_i^d(x, y) P_i(\lambda). \quad (1)$$

Because we are looking a bi-level image, gamma correction does not come into play.

The spectral sensitivity of the capture channels is denoted by $s_k(\lambda)$ where $k \in \{R, G, B\}$ represents the capture channels. The image captured by the camera can then be modeled as

$$I_k^c(x, y) = \int s_k(\lambda) r(x, y; \lambda) d\lambda, \quad (2)$$

where $k \in \{R, G, B\}$ and $I_k^c(x, y)$ represents the captured pixel corresponding to k^{th} camera capture channel. For simplicity of notation, we assume identical pixel co-ordinates for the displayed and captured images. In practice, synchronization methods that are part of barcode designs enables the captured barcode image to be registered to the encoded version. Now by substituting (1) in (2), relationship between captured pixel and displayed pixel is represented as

$$I_k^c(x,y) = \sum_{k,i} q_{ki} I_i^d(x,y), \tag{3}$$

where $q_{ki} = \int s_k(\lambda) P_i(\lambda) d\lambda$ represents amount that a display pixel $I_i^d(x,y)$ from i^{th} display channel contributes to the captured pixel $I_k^c(x,y)$ corresponding to k^{th} capture channel. Note that, in contrast with the per-channel printed barcodes considered in [10], the model for our per-channel display barcodes is inherently linear without requiring extensive simplifying assumptions. Hence if we know q_{ki} for $k \in \{R,G,B\}$ and $i \in \{R,G,B\}$, relation given in (3) allows us to perform the interference cancellation and estimate the display channels. The q_{ki} values can be represented as matrix $\mathbf{Q}$ where the i^{th} column is $[q_{Ri}, q_{Gi}, q_{Bi}]^T$. Hence, display channels $\mathbf{I^d} = [I_R^d, I_G^d, I_B^d]$ at a location (x,y) is obtained from the camera capture channels $\mathbf{I} = [I_R^c, I_G^c, I_B^c]$ at that location by

$$\mathbf{I^d} = \mathbf{Q^{-1} I^c}. \tag{4}$$

Using the above equation we can estimate the display channels. However, the matrix $\mathbf{Q}$ is usually unknown and we therefore propose two approaches to estimate the matrix that are analogous to those proposed in [10].

2.3. Color Interference Cancellation

a) Pilot Block Approach: In this method, the individual barcodes are designed *coherently* so that the synchronization patterns for these codes (and the data encoding modules) are aligned. The example of Fig.1 illustrates such a coherent design, where the finder patterns for the individual barcodes are aligned and the displayed color barcode shows a sample color pilot block allocation. The six pilot blocks present in the coherent barcode are combinations of the primaries used to create the color barcode i.e R, G, B, RG, RB, and GB. Because the blocks corresponding to the synchronization patterns do not carry any data, their colors can be selected at the encoder and the knowledge can be exploited at the decoder for estimating the cross channel interference matrix $\mathbf{Q}$. We refer to this as *pilot block* approach based on the similarity with pilot symbols for estimating channel state in communication systems [25].

In order to estimate the matrix $\mathbf{Q}$, the displayed pilot block barcode image is captured and R, G, B values at the pilot block positions are sensed which corresponds to I_R^c,I_G^c and I_B^c at those positions. Since the pilot blocks are the combinations of R, G, and B, the I_R^d,I_G^d and I_B^d are also known. In order to estimate the matrix $\mathbf{Q}$, the least squares method is adopted. After obtaining the matrix $\mathbf{Q}$, we use equation (4) to estimate $\mathbf{I^d}$ at every pixel. As a result we get three grayscale images corresponding to encoded estimates of the independent channels encoded in the color barcode.

Before feeding the interference canceled images to the decoder, it is necessary to binarize the images and hence we use adaptive thresholding (AT) technique to convert the grayscale image to binary image. Here, the intensity values at the pilot blocks are utilized and a threshold is set for each of the images. The thresholds are:

$$t_R = \frac{max(I_R^R, I_R^{RG}, I_R^{RB}) + min(I_R^G, I_R^B, I_R^{GB})}{2},$$
$$t_G = \frac{max(I_G^G, I_G^{RG}, I_G^{GB}) + min(I_G^R, I_G^B, I_G^{RB})}{2},$$
$$t_B = \frac{max(I_B^B, I_B^{RB}, I_B^{GB}) + min(I_B^R, I_B^G, I_B^{RG})}{2}, \tag{5}$$

where I_k^j represents intensity of k^{th} capture channel with $k \in \{R,G,B\}$ and j^{th} pilot block with $j \in \{R,G,B,RG,RB,GB\}$ and t_R, t_G, t_B represents the thresholds for each channel. The binary images are then fed to the decoder to decode the embedded data in each channel.

Algorithm 1: EM-type algorithm to estimate **Q**

Input : The captured color barcode
Output: **Q**
begin
Select k pixels in the captured image that has one of the R, G or B colors forming a $3 \times k$ matrix $\mathbf{I^c}$.
Initialize **Q**.
repeat
Set D to current estimate and minimize the objective function over $\mathbf{I^d}$;

$$\underset{\mathbf{I^d}}{minimize} \quad \left\|\mathbf{QI^d} - \mathbf{I^c}\right\|^2$$
$$subject\ to \quad 0 \leq \mathbf{I^d} \leq 1$$

Setting $\mathbf{I^d}$ to current estimate ,minimize the objective function over **Q**

$$\underset{\mathbf{Q}}{minimize} \quad \left\|\mathbf{QI^d} - \mathbf{I^c}\right\|^2$$
$$subject\ to \quad 0 \leq \mathbf{Q}$$

until $\left\|\mathbf{QI^d} - \mathbf{I^c}\right\|^2 < \tau$ *i.e until objective function is less than the threshold* τ;
end

b) EM-type approach: This algorithm does not require a coherent design for the barcodes (See Fig.2 for incoherent encoding example). It is an iterative algorithm where we can estimate $\mathbf{I^d}$ and $\mathbf{Q}$ simultaneously. $\mathbf{I^d}$ is treated as variable constrained between 0 and 1 and can be interpreted as the probabilities of R, G, and B primaries getting displayed at a particular pixel location on screen. The matrix $\mathbf{Q}$ is constrained to have only positive entries. The objective function to be minimized is $\left\|\mathbf{QI^d} - \mathbf{I^c}\right\|^2$. This results in an optimization problem where we alternately estimate $\mathbf{I^d}$ and $\mathbf{Q}$ in such a way that the objective function is minimized. Since $\mathbf{I^d}$ and $\mathbf{Q}$ are present in the objective function it can implemented as alternating constrained least squares as indicated in Algorithm 1. In this algorithm, $\mathbf{I^c}$, which represents a captured pixel, is chosen from a subset of pixels from the captured barcode. Hence $\mathbf{I^c}$ represents a $3 \times k$ matrix for k pixels chosen from the image. To initialize matrix $\mathbf{Q}$, the captured image is Otsu thresholded [26] and we use least squares to obtain initial estimate of $\mathbf{Q}$. With initialization of $\mathbf{Q}$ and $0 \leq \mathbf{I^d} \leq 1$ as constraint, $\mathbf{I^d}$ is estimated. Using the estimated $\mathbf{I^d}$ and $\mathbf{Q} \geq 0$ as constraint we estimate the matrix $\mathbf{Q}$. The procedure continues until the objective function minimizes below the predetermined threshold τ. After obtaining the matrix $\mathbf{Q}$, equation (4) is used to estimate the display color channels $\mathbf{I^d}$ at every location. In order to binarize the estimated channels we use the Otsu thresholding method [26] and feed the binary images to the decoder.

Pilot block approach is employed for coherent barcode designs whereas EM type approach can be used to recover the data from both coherent and incoherent color barcodes. Incoherent color barcodes (see Fig.2) have different data lengths and the alignment and synchronization patterns in each channel need not be aligned. Hence the EM type approach is advantageous in case of incoherently encoded color barcodes.

3. EXPERIMENTAL RESULTS

For our experiments, we chose the QR code and Aztec code because they are widely used in mobile applications. Color versions of these codes were generated in the proposed per-channel framework in three different sizes: 30, 40, and 50mm and using two different error correction levels, L and Q, specified in the standards [2, 3]. Both coherent and incoherent designs of the codes were utilized in the experiments, where the coherent designs use the synchronization markers as pilot blocks as described in Section 2. These barcodes were displayed on two displays and captured using four different smartphones. The resulting images were then separated into the individual R, G, and B channels which were used in the barcode decoding process, either directly after Otsu thresholding (OT) [26], or after interference cancellation using (for the coherently designed codes) the pilot block (PB+AT) approach or (for both the coherent and incoherent designs) the EM approach. For the EM approach the threshold was set as $\tau = 10^{-5}$.

To evaluate performance of the algorithms we use Bit Error Rate (BER) and Decoding Success Rate (DSR) as the performance metrics. BER is the percentage of bits in error, in the recovered bit stream when compared to original bit stream prior to error correction decoding and DSR represents percentage of captured barcodes decoded successfully using the error correction decoding (for the Reed-Solomon codes used). Because of space-limitations, we present only aggregate statistics highlighting our main findings. Figures 4, 5, and 6 summarize the percentage BER for three barcode sizes for the R, G, and B channels, respectively. In each channel and for each size of the color barcode, three bars represent the percentage BER for OT, PB+AT, and EM methods in order from left to right. We can observe that even without the interference cancellation the BER is less than 1.23% for the OT method and the interference cancellation reduces the BER further for both the PB+AT and EM methods, especially for the green channel where cross channel interference is higher compared to other channels. The PB+AT method usually performs slightly better that the EM method. Assuming a binary symmetric channel and 1.23% BER, which is an upper bound for our observed error rates, the estimated capacity of our color barcode scheme is 3×0.9043 bits per encoded module which is quite close to the maximum of 3 achievable with the framework. With interference cancellation the BER's are all below 0.31% providing an estimated capacity of 3×0.9697 bits per module. While the low BER's obtained with OT without any interference cancellation are usually readily handled by the error correction codes utilized, the further reduction in BER's provided by interference cancellation is advantageous when errors are also introduced from other sources; for instance, for artistic and branding purposes [27] deliberate distortions are introduced in barcodes. The interference cancellation ensures better robustness in the face of such deliberate distortions. Table 1 compares the DSR for OT, PB+AT, and EM methods where the ratios represent number of successfully decoded cases to total number of cases. The benefit of interference cancellation is apparent from the results in the third and fourth row of Table 1 compared to the second row.

DSR comparison	R	G	B
OT	48/54	50/58	47/53
PB+AT	49/52	53/56	49/51
EM	35/39	46/46	39/40

Table 1: Decoding Success Rate comparison for OT, PB+AT, and EM methods for the R, G and B channels.

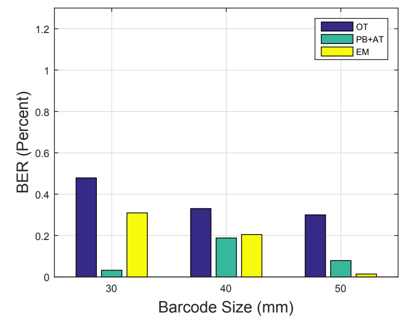

Fig. 4: BER vs Barcode size for the R channel

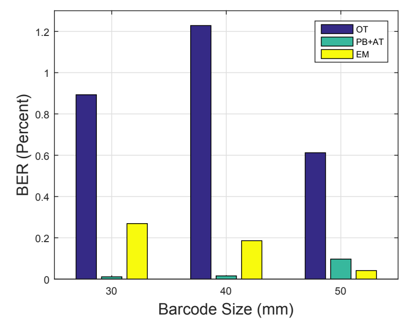

Fig. 5: BER vs Barcode size for the G channel

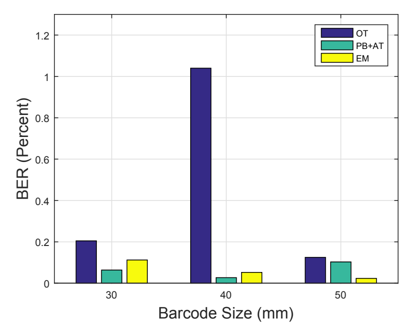

Fig. 6: BER vs Barcode size for the B channel

4. CONCLUSION AND DISCUSSION

In this paper, we present a per-channel color barcode framework for display applications. We show analytically that cross channel interference for our framework is quite small and can be further reduced via interference estimation and cancellation using either: the synchronization regions in coherently designed individual channel barcodes or via expectation maximization, which also applies to incoherent encoding of individual channel barcodes. In a battery of tests across multiple displays and smartphones, using both QR and Aztec codes, the raw bit error rate prior to forward error correction (FEC) are under 1.23% for our framework and further reduced by interference cancellation. These errors are readily corrected using the FEC built into common barcodes such as the Reed-Solomon codes for the QR and Aztec codes. While the interference cancellation is not required when capturing pristine color barcodes, it provides additional headroom for errors that are deliberately introduced through aesthetic modifications.

5. REFERENCES

[1] ISO/IEC, "Information technology – Automatic identification and data capture techniques – EAN/UPC bar code symbology specification," http://www.iso.org/iso/iso_catalogue/catalogue_ics/catalogue_detail_ics.htm?csnumber=46143, 2009, accessed Jan 2011.

[2] ——, "Information technology – Automatic identification and data capture techniques – QR Code 2005 bar code symbology specification," http://www.iso.org/iso/iso_catalogue/catalogue_ics/catalogue_detail_ics.htm?csnumber=43655, 2006, accessed Jan 2011.

[3] ——, "Information technology – Automatic identification and data capture techniques – Aztec Code bar code symbology specification," http://www.iso.org/iso/iso_catalogue/catalogue_tc/catalogue_detail.htm?csnumber=41548, 2008, accessed Apr 2011.

[4] A. Longacre and R. Hussey, "Two dimensional data encoding structure and symbology for use with optical readers," United States Patent 5,591,956, 7 Jan. 1997.

[5] C. Sant'Anselmo, R. Sant'Anselmo, and D. C. Hopper, "Identification symbol system and method with orientation mechanism," United States Patent 5,612,524, Mar. 1997.

[6] T. Hao, R. Zhou, and G. Xing, "COBRA: Color barcode streaming for smartphone systems," in *Procs. of the 10th Int. Conf. on Mobile Sys., App., and Services*, ser. MobiSys '12. New York, NY, USA: ACM, 2012, pp. 85–98. [Online]. Available: http://doi.acm.org/10.1145/2307636.2307645

[7] D. Parikh and G. Jancke, "Localization and segmentation of a 2D high capacity color barcode," in *IEEE Workshop on Applications of Computer Vision (WACV)*, Copper Mountain, CO, USA, Jan. 2008, pp. 1–6.

[8] O. Bulan, H. Blasinski, and G. Sharma, "Color QR codes: Increased capacity via per-channel data encoding and interference cancellation," in *Proc. IS&T/SID Nineteenth Color and Imaging Conference: Color Science and Engineering Systems, Technologies, and Applications*, San Jose, CA, 7-11 Nov. 2011, pp. 156–159.

[9] R. John and K. Raahemifar, "Designing a 2D color barcode," in *28th IEEE Canadian Conf. on*, May 2015, pp. 297–301.

[10] H. Blasinski, O. Bulan, and G. Sharma, "Color barcodes for mobile applications: A per channel framework," *IEEE Trans. Image Proc.*, vol. 22, no. 4, pp. 1498–1511, Apr. 2013.

[11] G. Sharma, "Image-based data interfaces revisited: Barcodes and watermarks for the mobile and digital worlds," in *8th Intl. Conf. on Comm. Sys. and Networks (COMSNETS)*, Bangalore, India, Jan. 2016.

[12] M. Rohs, "Real-world interaction with camera phones," in *Ubiquitous Computing Systems*. Springer, 2005, pp. 74–89.

[13] D. Scott, R. Sharp, A. Madhavapeddy, and E. Upton, "Using visual tags to bypass bluetooth device discovery," *SIGMOBILE Mob. Comput. Commun. Rev.*, vol. 9, no. 1, pp. 41–53, 2005. [Online]. Available: http://doi.acm.org/10.1145/1055959.1055965

[14] M. Fetter, C. Beckmann, and T. Gross, "Magneticode: Physical mobile interaction through time-encoded magnetic identification tags," in *Procs. of the 8th Intl. Conf. on Tangible, Embedded and Embodied Interaction*, ser. TEI '14. New York, NY, USA: ACM, 2013, pp. 205–212. [Online]. Available: http://doi.acm.org/10.1145/2540930.2540963

[15] B. Zhang, K. Ren, G. Xing, X. Fu, and C. Wang, "SBVLC: Secure barcode-based visible light communication for smartphones," in *IEEE INFOCOM Procs.*, Apr. 2014, pp. 2661–2669.

[16] "Walmart launches mobile payments processor." http://www.businessinsider.com/walmart-launches-mobile-payments-processor-2015-12?IR=T, Posted on Dec. 14, 2015 in Business Insider.

[17] "Wal-mart adds to mobile wallet frenzy with walmart pay." http://www.reuters.com/article/us-wal-mart-mobilepayment-idUSKBN0TT0E620151210, Posted on Dec. 10, 2015 in Reuters.

[18] ISO/IEC, "ISO/IEC 18092:2013 Information technology – Telecommunications and information exchange between systems – Near Field Communication – Interface and Protocol (NFCIP-1)," 2013. [Online]. Available: http://standards.iso.org/ittf/PubliclyAvailableStandards/c056692_ISO_IEC_18092_2013.zip

[19] K. Finkenzeller, *RFID Handbook: Radio-frequency identification fundamentals and applications*. Wiley, 1999.

[20] ISO/IEC, "ISO/IEC 15693-1:2010 Identification cards – Contactless integrated circuit cards – Vicinity cards – Part 1: Physical characteristics," 2010. [Online]. Available: http://www.iso.org/iso/home/store/catalogue_tc/catalogue_detail.htm?csnumber=39694

[21] ——, "ISO/IEC 14443-1:2008 Identification cards – Contactless integrated circuit cards – Proximity cards – Part 1: Physical characteristics." [Online]. Available: http://www.iso.org/iso/home/store/catalogue_tc/catalogue_detail.htm?csnumber=39693

[22] T. Langlotz and O. Bimber, "Unsynchronized 4D barcodes," in *Advances in Visual Computing*. Springer, 2007, pp. 363–374.

[23] O. Bulan and G. Sharma, "Improved color barcodes via expectation maximization style interference cancellation," in *Proc. IEEE Intl. Conf. Acoustics Speech and Sig. Proc.*, Kyoto, Japan, Mar. 2012, pp. 1509–1512.

[24] G. Sharma, "LCDs versus CRTs-color-calibration and gamut considerations," *Procs. of the IEEE*, vol. 90, no. 4, pp. 605–622, Apr. 2002.

[25] J. G. Proakis and M. Salehi, *Digital communications*. McGraw-Hill, 2008.

[26] N. Otsu, "A threshold selection method from gray-level histograms," *Automatica*, vol. 11, no. 285-296, pp. 23–27, 1975.

[27] Z. Baharav and R. Kakarala, "Visually significant QR codes: Image blending and statistical analysis," in *IEEE Intl. Conf. on Multimedia and Expo (ICME), 2013*, Jul. 2013, pp. 1–6.